Atmos. Chem. Phys. Discuss., 11, 10693–10720, 2011
www.atmos-chem-phys-discuss.net/11/10693/2011/
doi:10.5194/acpd-11-10693-2011
© Author(s) 2011. CC Attribution 3.0 License.

Atmospheric Chemistry and Physics Discussions

This discussion paper is/has been under review for the journal Atmospheric Chemistry and Physics (ACP). Please refer to the corresponding final paper in ACP if available.

Yields of oxidized volatile organic compounds during the OH radical initiated oxidation of isoprene, methyl vinyl ketone, and methacrolein under high–NO_x conditions

M. M. Galloway[1], A. J. Huisman[1,*], L. D. Yee[2], A. W. H. Chan[3,], C. L. Loza[3], J. H. Seinfeld[2,3], and F. N. Keutsch[1]**

[1]Department of Chemistry, University of Wisconsin–Madison, Madison, WI, USA
[2]Division of Engineering and Applied Science, California Institute of Technology, Pasadena, CA, USA
[3]Division of Chemistry and Chemical Engineering, California Institute of Technology, Pasadena, CA, USA
[*]now at: Institute for Atmosphere and Climate, ETH Zurich, Zurich, Switzerland
[**]now at: Department of Environmental Science, Policy and Management, University of California, Berkeley, CA, USA

Received: 29 March 2011 – Accepted: 30 March 2011 – Published: 6 April 2011

Correspondence to: F. N. Keutsch (keutsch@wisc.edu)

Published by Copernicus Publications on behalf of the European Geosciences Union.

Abstract

We present first-generation and total production yields of glyoxal, methylglyoxal, glycolaldehyde, and hydroxyacetone from the oxidation of isoprene, methyl vinyl ketone (MVK), and methacrolein (MACR) with OH under high NO_x conditions. Several of these first-generation yields are not included in commonly used chemical mechanisms, such as the Leeds Master Chemical Mechanism (MCM) v. 3.1. Inclusion of first-generation production of glyoxal, glycolaldehyde and hydroxyacetone from isoprene and methylglyoxal from MACR greatly improves performance of an MCM based model during the initial part of the experiments. In order to further improve performance of the MCM based model, higher generation glyoxal production was reduced by lowering the first-generation yield of glyoxal from C5 carbonyls. The results suggest that glyoxal production from reaction of OH with isoprene under high NO_x conditions can be approximated by inclusion of a first-generation production term together with secondary production only via glycolaldehyde. Analogously, methylglyoxal production can be approximated by a first-generation production term from isoprene, and secondary production via MVK, MACR and hydroxyacetone. The first-generation yields reported here correspond to less than 5% of the total oxidized yield from isoprene and thus only have a small effect on the fate of isoprene. However, due to the abundance of isoprene, the combination of first-generation yields and reduced higher generation production of glyoxal from C5 carbonyls is important for models which include the production of the small organic molecules from isoprene.

1 Introduction

Isoprene (2-methyl-1,3-butadiene) is emitted into the atmosphere from vegetation in large quantities (~500 Tg year^{-1}) (Guenther et al., 1995). Globally, the dominant atmospheric sink of isoprene is reaction with the OH radical (Archibald et al., 2010a). Due to its reactivity with the OH radical and high mixing ratios in forested areas, isoprene has

ACPD
11, 10693–10720, 2011

important impacts on the oxidative capacity of the atmosphere (Karl et al., 2009). OH oxidation of isoprene has been studied in detail, and there are a number of commonly used mechanisms such as the Leeds Master Chemical Mechanism (MCM), Mainz Isoprene Mechanism (MIM) or the NCAR Master Chemical Mechanism (Madronich and Calvert, 1989; Jenkin et al., 2003; Saunders et al., 2003; Taraborrelli et al., 2009). Oxidation of isoprene initiated by OH is an important source of small carbonyls and hydroxycarbonyls, such as glyoxal, methylglyoxal, and glycolaldehyde. These species are of great interest within the context of cloud processing and secondary organic aerosol (SOA) formation (Carlton et al., 2007; Altieri et al., 2008; Ervens et al., 2008; Galloway et al., 2009; Ip et al., 2009; Nozière et al., 2009; Perri et al., 2009; Shapiro et al., 2009; Tan et al., 2009; Volkamer et al., 2009; Sareen et al., 2010). To quantify the atmospheric impacts of these compounds, it is important to understand their tropospheric production via oxidation of volatile organic compounds (VOCs), isoprene in particular.

Atmospheric isoprene oxidation has long been of interest (Gu et al., 1985; Tuazon and Atkinson, 1990a; Paulson et al., 1992; Miyoshi et al., 1994; Kwok et al., 1995; Sprengnether et al., 2002; Fan and Zhang, 2004; Zhao et al., 2004; Carlton et al., 2009; Karl et al., 2009; Paulot et al., 2009a; Archibald et al., 2010a,b). Tuazon and Atkinson (1990a) studied isoprene oxidation in the presence of OH and NO_x, and determined first-generation formation yields of methyl vinyl ketone (MVK), methacrolein (MACR), and formaldehyde. The same authors also determined first-generation photooxidation yields of glycolaldehyde and methylglyoxal from MVK as well as yields of hydroxyacetone, methylglyoxal, and CO from MACR (Tuazon and Atkinson, 1989, 1990b). Orlando et al. (1999) studied OH–initiated MACR oxidation in the presence of NO_x and quantified hydroxyacetone as a product. They did not observe first-generation production of methylglyoxal; based on their detection limit for methylglyoxal, they determined an upper limit of 12% for the first-generation methylglyoxal yield from MACR.

While all of these studies have added to our mechanistic understanding of isoprene oxidation, recent measurements point to gaps in our understanding of isoprene oxidation (Dibble, 2004a,b; Volkamer et al., 2006; Paulot et al., 2009a). The existing master

ACPD
11, 10693–10720, 2011

mechanisms cited above specify glyoxal as a higher generation oxidation product of isoprene, but few studies exist in which glyoxal is measured in isoprene oxidation. One such study compared first-generation MACR and glyoxal to derive a first-generation glyoxal yield of 0.3–3% (Volkamer et al., 2006). Theoretical work by Dibble (2004a,b) suggests a mechanism for such first-generation glyoxal and methylglyoxal formation from isoprene under high NO_x conditions, specifically that glyoxal, methylglyoxal, glycolaldehyde, and hydroxyacetone can be formed through rapid isomerisation and double intramolecular hydrogen transfer of alkoxy radical intermediates. Glycolaldehyde and methylglyoxal are produced together in the suggested mechanism, as are glyoxal and hydroxyacetone. Paulot et al. (2009a) also studied isoprene oxidation, focusing on the isoprene δ–hydroxy oxidation channel. They observed first-generation yields of glycolaldehyde and hydroxyacetone and inferred the same yields for methylglyoxal and glyoxal, respectively, based on the work of Dibble (2004a,b) as they had no measurements of the dicarbonyls.

The work presented here studies the formation of a number of first– and higher–generation products formed during OH oxidation of isoprene, MVK, and MACR under high NO_x conditions. First–generation yields from these precursors are incorporated into a zero–dimensional photochemical box model based on the MCM v. 3.1 (Madronich and Calvert, 1989; Jenkin et al., 2003; Saunders et al., 2003; Taraborrelli et al., 2009; Huisman et al., 2011) to evaluate the extent to which the model can represent experimental measurements.

2 Experimental procedures

Experiments were carried out in the Caltech dual 28 m^3 Teflon chambers, described in detail elsewhere (Cocker et al., 2001; Keywood et al., 2004). See Table 1 for experimental conditions. Temperature, relative humidity (RH), O_3, NO, and NO_x were continuously monitored. RH was held at ~10% throughout the experiments. Gas–phase isoprene, MVK, and MACR were monitored by gas chromatography with a flame ionization detector (GC–FID, Agilent 6890N).

ACPD
11, 10693–10720, 2011

Gas–phase glyoxal was continuously monitored using the Madison laser induced phosphorescence instrument described by Huisman et al. (2008). This instrument has 30 s time resolution, with a limit of detection (3σ) for glyoxal of 16 ppt s^{-1}. Methylglyoxal was also measured with this instrument by subtracting glyoxal and background signals from the total α–dicarbonyl signal to give the methylglyoxal signal. Calibrations are performed with the same methods described for glyoxal by Huisman et al. (2008). Exp. 1, 7, and 9 (Table 2) also utilized the lifetime methylglyoxal detection method described by Henry et al. (2011).

A chemical ionization mass spectrometer (CIMS) was used for online gas–phase measurement of glycolaldehyde and hydroxyacetone. The CIMS consists of a custom chemical ionization source connected to a Varian 1200 triple quadrupole mass spectrometer, previously described in detail (Crounse et al., 2006; Paulot et al., 2009b; St. Clair et al., 2010). Negative–mode operation utilized CF_3O^- ions that cluster with the analyte seen at *m/z* MW + 85 or via fluoride transfer for more acidic species seen at *m/z* MW + 19. Positive–mode operation utilized proton transfer reaction of positively charged water clusters with the analyte.

Experiments typically began with the addition of the reactants into the chamber. A known amount of liquid isoprene, MVK, or MACR was injected into a glass bulb, vaporised into the chamber, and then allowed to mix. Photolysis of nitrous acid (HONO) was used as the OH precursor. HONO was prepared by adding 1 wt% aqueous $NaNO_2$ drop wise into 10 wt% sulphuric acid and then introduced into the chamber using an air stream. Additional NO was added. Experiment time started when the blacklights were turned on.

3 Determination of first-generation yields

Observed mixing ratios reflect both production and loss of each compound. To calculate total production yields, it is necessary to correct for the amount of product lost via photolysis and reaction with OH and O_3. This requires knowledge of the reaction rates

ACPD
11, 10693–10720, 2011

with OH (k_{OH+X}) and O_3 (k_{OH+X}) (taken from the MCM), the O_3 concentration (which was measured), the photolysis rates (inferred from the measured glyoxal photolysis rate, see Sect. 3.1), as well as the OH concentration (inferred from the rate of change of observed VOCs, see Sect. 3.2).

3.1 Calculating photolysis rates

The glyoxal photolysis rate was measured during the 2008 experiments (Exp. C1, Chan et al., 2009) and again during the 2010 experiments (Exp. 1) to account for changes in blacklight intensity. Glyoxal photolysis in 2010 ($0.14\,h^{-1}$) was 74% of the value in 2008 ($0.19\,h^{-1}$), so the 2009 photolysis rate was interpolated between these values. The photolysis rates calculated from these experiments were used as a basis to estimate the photolysis rates of all other compounds. Photolysis rates in the MCM are given as a function of solar zenith angle (SZA), so the measured glyoxal photolysis rate was used to calculate an estimated SZA from the MCM; this was then used to calculate the photolysis rates for all other species.

3.2 Determining OH concentrations

OH number densities were estimated from the rate of loss of VOCs. Loss of VOC via reaction with O_3 and photolysis was taken into account by iteratively solving the loss equation for the precursor VOC, rearranged to solve for [OH],

$$[OH] = -\frac{1}{k_{OH+X}}\left(\frac{1}{[X]_{i-1}}\frac{\Delta[X]}{\Delta t} + k_{O_3+X}[O_3]_i + J_X\right) \quad (1)$$

where [X] is the number density of the VOC, $[X]_{i-1}$ is the measured product concentration of measurement i-1, $\frac{\Delta[X]}{\Delta t}$ is the change in number density per unit time, k_{OH+X} and k_{O_3+X} are the rate constants for reaction with OH and O_3, respectively, and J_X is the photolysis rate. The precursor VOC number densities were smoothed, in order to reduce scatter in the OH data. For the isoprene experiments, OH was calculated from

ACPD
11, 10693–10720, 2011

isoprene until isoprene number density dropped below the limit of detection of the GC–FID, after which smoothed MVK and MACR data were used. OH was determined to be the mean of that calculated from MVK and MACR at each step. OH was calculated to be 1×10^6–1×10^7 molec cm^{-3} at the start of the experiment and decreased to 1×10^4 molec cm^{-3} towards the end of the experiments.

3.3 Loss correction

Number densities of each product corrected to account for reaction with OH and O_3, $[Y]^{corr}$, were determined iteratively using the following recursive discrete time equation:

$$[Y]_i^{corr} = [Y]_{i-1}^{corr} + \Delta[Y]_i + [Y]_{i-1}\Delta t(k_{OH+Y}[OH] + k_{O_3+Y}[O_3] + J_Y]) \quad (2)$$

where $[Y]_i^{corr}$ is the corrected number density of the compound at measurement time i, $[Y]_{i-1}$ is the measured product concentration of measurement i-1, Δt is time between measurements i and i-1, $\Delta[Y]_i$ is the change in [Y] that occurs over Δt, k_{OH+Y} and k_{O_3+Y} are the respective rate constants, and J_Y is the photolysis rate constant of the product Y. At any given time during the experiment, $[Y]^{corr}$ is equivalent to the total amount of Y which was produced up to that point, neglecting all loss processes.

3.4 First–generation yields

The relationship between the loss corrected concentrations of reaction products and the amount of precursor VOC consumed via reaction is an indicator of first-versus higher-generation formation. VOCs react with OH, forming peroxy radicals, which then react largely with NO, giving alkoxy radicals and other species. First-generation reactions are those that stem from the initial OH attack and which do not involve another attack by OH, O_3, or NO_3 on one of the stable products. Therefore, a first generation product is the first stable product which results from one OH reacting with the precursor VOC. This first generation product is formed at the same rate at which the precursor VOC is lost to reaction, therefore the relationship between these quantities would be

ACPD
11, 10693–10720, 2011

linear. In contrast, a lag in the appearance of the product demonstrates that the reaction involves intermediates, as production does not depend on the reaction of the primary VOC but rather on that of a first or later generation product. The slope of the line observed for the loss corrected concentration versus reacted VOC corresponds to the first-generation yield (Fig. 1a). In contrast to isoprene, this linear region is relatively short for MVK and MACR as a result of the relative lifetimes of first-generation products compared to those of MVK and MACR (Fig. 1b). For these cases, the corrected product data are fit to an exponential with a linear component:

$$[Y]=a\Delta[X]+be^{c\Delta[X]}-b \tag{3}$$

where a is the first-generation yield of the product ([Y]) from the precursor VOC ([X]), and b and c take into account second and later generation production. First–generation yields were determined for each of the measured oxidation products in these experiments using the methods described above (Table 3). A representative isoprene oxidation experiment is shown in Fig. 1; the first-generation glyoxal yield calculated from this experiment is $(2.32 \pm 0.01)\%$. The first-generation yields of MVK and MACR from isoprene presented here agree well with Tuazon and Atkinson (1990a). The first-generation glyoxal yield from isoprene calculated from our work is in the upper range (0.3–3%) presented by Volkamer et al. (2006). Of the species studied here, the MCM includes only first-generation formation of MVK and MACR from isoprene, for which the yields are also shown in Table 3. Although first-generation formation of the two and three carbon species listed in Table 3 from isoprene is not included in the MCM or other common mechanisms, Dibble (2004a,b) has presented a possible reaction pathway in a theoretical study. The Dibble mechanism rationalizes first-generation formation of glyoxal together with hydroxyacetone and first-generation formation of methylglyoxal together with glycolaldehyde from isoprene via intramolecular hydrogen shift reactions of the radical intermediates in the presence of NO. Although our methylglyoxal observations are inconclusive, the glyoxal, glycolaldehyde and hydroxyacetone observed in the work presented here agrees with this, as does the work by Paulot et al. (2009a),

ACPD
11, 10693–10720, 2011

who also observed first-generation production of glycolaldehyde and hydroxyacetone from reaction of isoprene and OH with similar yields.

The first-generation yields of glycolaldehyde and methylglyoxal from MVK in this study agree within error to those found by Tuazon and Atkinson (1989). The same authors also determined a first-generation yield for hydroxyacetone from MACR (Tuazon and Atkinson, 1990b); our yield is on the high end of this range, but is in good agreement with the yield determined by Orlando et al. (1999). The first-generation yield of methylglyoxal from MACR in this work is lower but similar to that determined by Tuazon and Atkinson (1989), whereas the yield inferred by Paulot et al. (2009a) is substantially higher. Overall, the first-generation yields determined in this work agree with previously reported literature values.

4 Comparison of first and higher generation yields with the MCM

4.1 MCM based model parameters

The MCM based photochemical box model described in detail by Huisman et al. (2011) was used to reproduce chamber results with minor modifications to the model parameters. O_3, NO_2, and air temperature were constrained to match measurements. However, for these chamber runs, the primary VOC and NO concentrations were not constrained to the measurements but predicted by the model after initialization with the observed initial values. Two features of the box model are the use of an SZA derived from measured photolysis rates (Sect. 3.1) and the use of chamber–derived OH (Sect. 3.2). Raw NO_2 data were corrected for detector saturation ($[NO_2] > 1000$ ppb_v) using a cubic spline fitting routine. In very dry, low aerosol conditions such as those in these experiments, glyoxal has been demonstrated to have negligible wall losses, and wall and aerosol losses are expected to be a minor to negligible sink of the other VOCs as well (Loza et al., 2010). Therefore, wall and aerosol losses are neglected in the model.

ACPD
11, 10693–10720, 2011

4.2 Assessment of unmodified MCM

Model performance is assessed using a quality of fit parameter that takes into account the slope, correlation coefficient (R^2), and absolute residuals between measurement and model. The fit is evaluated for a short time, usually less than 1 hour after experiment start, which reflects primarily first-generation production, and evaluated again for the remainder of the experiment, corresponding to a convolution of first and higher generation production. For the purposes of this assessment, first-generation production is defined as experiment start until the instantaneous production rate of a representative first-generation compound (e.g. MVK for an isoprene experiment, glycolaldehyde for MVK) is one-quarter of the initial instantaneous production rate. After this time, the experiment is considered to be in the higher generation production regime. The slope of the fit between measurement and model is used to determine the bias in the model.

The MCM based model was able to reproduce chamber results for oxidation of MBO upon inclusion of the 29% yield of glyoxal from glycolaldehyde found by Chan et al. (2009). For the high–NO_x isoprene oxidation experiments, the model predicted MVK and MACR well. In contrast, the model underpredicted glyoxal (Fig. 2), methylglyoxal, hydroxyacetone, and glycolaldehyde in the primary production regime. This demonstrates that, as expected from Sect. 3, a first-generation yield is necessary to bring the model into agreement with measurements in the early part of the experiments. In contrast, the model overpredicts glyoxal in the later, higher generation production regime by approximately a factor of two.

For the MVK high–NO_x oxidation experiments, predicted glyoxal (Fig. 3) agrees very well with measurement, and modelled glycolaldehyde only slightly exceeds the measurements. Measured methylglyoxal concentrations are approximately double modelled concentrations at later experimental times. Predicted hydroxyacetone agrees well with measurement for the high NO_x MACR experiment, but modelled methylglyoxal is approximately 50% less than measured.

ACPD
11, 10693–10720, 2011

4.3 Inclusion of first-generation yields in MCM model

The first-generation yields determined in Sect. 3.2 and Table 2 that are not included in the current version of the MCM were added to the MCM–based model, i.e. first-generation production of glyoxal, glycolaldehyde, hydroxyacetone and methylglyoxal from isoprene and first-generation methylglyoxal production from MACR. As our results for first-generation formation of methylglyoxal from isoprene were inconclusive, we used the same value as that determined for glycolaldehyde following the work of Dibble (2004a,b) and Paulot et al. (2009a). Figure S4 shows the details of the modifications made to the MCM. The yields of hydroxyacetone, glycolaldehyde and glyoxal are quite similar to those observed (or inferred for the case of glyoxal) by Paulot et al. (2009a) with exception of the first-generation yield of methylglyoxal from MACR, which is substantially lower in our work than the inferred value.

The unaltered MCM based model and a model with the first-generation yields were used to simulate chamber experiments of oxidation of isoprene, MVK, and MACR. Inclusion of the first-generation yields improved the model performance at early times in the isoprene and MACR studies (see Fig. 2 for a representative example), clearly supporting the finding that these first-generation formation pathways should be incorporated into chemical mechanisms.

4.4 Attenuation of higher generation glyoxal production in the MCM

While the inclusion of first-generation production of glyoxal allowed the model to match early experimental results, the model still had a substantial over prediction at later times ($t > 1$ h) when the majority of isoprene had already been processed, which implies that glyoxal as a higher generation oxidation product of isoprene is significantly over expressed in the MCM for the conditions of our chamber experiments. There are several channels that produce glyoxal (see Fig. 4), most of which have been studied in detail; the glyoxal yield from glycolaldehyde is known and glycolaldehyde was reproduced well in the later part of experiments, first-generation production of glyoxal

ACPD
11, 10693–10720, 2011

from isoprene was determined experimentally, and the model is able to adequately reproduce glyoxal from both MVK and MACR oxidation experiments. The discrepancies in glyoxal production from isoprene oxidation are hence unlikely to result from any of these channels (Fig. 4). The majority of glyoxal not produced through these channels is formed through C5 carbonyls (Fig. 4); therefore we adjusted the yield of glyoxal from C5 carbonyls in the MCM. Using the observed first-generation yield for glyoxal in the isoprene experiments, a model variant in which production of glyoxal from C5 carbonyls was eliminated improved model performance markedly (Fig. 2). By removing the higher generation production of glyoxal from C5 carbonyls, most of the glyoxal production from isoprene oxidation can be modelled through first-generation formation from isoprene and the oxidation of glycolaldehyde. Glyoxal production from C5 carbonyls is not necessarily wrong in the MCM; there are several other reasons why this attenuation might improve model performance. These include a missing C5 carbonyl sink, incorrect reaction rates to form glyoxal, or C5 carbonyl wall loss in the chambers. Attenuating the glyoxal production from these compounds is the easiest to achieve in this study, and further experiments to study C5 carbonyl formation and oxidation are necessary to fully understand glyoxal production from isoprene.

Even with C5 carbonyl attenuation, modelled glyoxal is still slightly higher than measurements (Fig. 2), and the model modifications addressed above do not bring the measurement and model into perfect agreement. This could be due to the fact that OH is not measured, but is calculated from the isoprene, MVK, and MACR decay.

4.5 Total product yields from the MCM

Once the model parameters were set to reproduce the measured species of interest, the altered MCM–based model was used to determine total yields of each of the products studied from isoprene, MVK, and MACR. To do this, the OH, O_3, NO_2, and air temperature inputs were extended at the final measured value and the model was allowed to run until all products of interest were consumed. The total amount of each

ACPD
11, 10693–10720, 2011

compound produced was compared to the total consumption of the precursor VOC. The results of these model runs are shown in Table 3.

5 Conclusions

We present yields of first-generation oxidation products of isoprene, MVK, and MACR, several of which are not included in current chemical mechanisms, such as the MCM. Inclusion of first-generation production of glyoxal, glycolaldehyde and hydroxyacetone from isoprene and methylglyoxal from MACR greatly improves performance of a MCM based model during the first few hours of oxidation. However, inclusion of the first-generation glyoxal yield degraded the already poor performance of the MCM based model during the higher generation production phase of the isoprene experiments. It was necessary to scale down higher generation glyoxal production from isoprene in order to prevent substantial overprediction in relation to chamber experiments. Reducing the glyoxal production from C5 carbonyls greatly improves model performance, indicating that this pathway could be overexpressed in the MCM. However, further work is needed to determine whether the cause of the over prediction is indeed from the fate of C5 carbonyls, which could not be ascertained in this work, as no experiments with the C5 carbonyls themselves were conducted; in addition, the high glyoxal yield from glycolaldehyde in this study should be verified.

The results presented here furthermore suggest that glyoxal production from reaction of OH with isoprene under high NO_x conditions can be approximated by inclusion of only a first-generation production term together with secondary production via glycolaldehyde, which simplifies the MCM isoprene mechanism for glyoxal. Similarly, we propose that methylglyoxal production can be approximated by a first-generation production term from isoprene, and secondary production via MVK, MACR and hydroxyacetone (Fig. 4).

ACPD
11, 10693–10720, 2011

Atmospheric implications

The first-generation yields of glyoxal, methylglyoxal, hydroxyacetone, and glycolaldehyde correspond to less than 5% of the total isoprene yield and thus only have a small effect on the overall fate of isoprene. However, due to the abundance of isoprene, these findings together with the reduced higher generation production of glyoxal from C5 carbonyls are important for models that investigate the production of the small oxidized organic molecules, especially within the context of SOA formation and cloud processing. If current models overestimate gas–phase glyoxal mixing ratios in areas dominated by isoprene by a factor of 2–6 (as seen in this study), then SOA production from glyoxal could be overestimated to a similar degree. Fu et al. (2008, 2009) used the GEOS–Chem global model updated with oxidation chemistry from the MCM to determine global aerosol yields from glyoxal and methylglyoxal. The global annual mean yields of glyoxal and methylglyoxal from OH reaction with isoprene as calculated by GEOS–Chem were 8% and 29%, respectively, significantly higher than the total yields reported in this work. Subtraction of the glyoxal yield via C5 carbonyls (3.78%) from the total glyoxal yield predicted by GEOS–Chem results in a higher–generation glyoxal yield from isoprene of 4.22%. With the addition of this yield to the first-generation glyoxal yield from isoprene in this study (2.1%), an overall glyoxal yield of 6.3% from OH reaction with isoprene is predicted. This yield is very close to that found in this study. Stavrakou et al. (2009) estimated a range of glyoxal yields from isoprene of 7.2–35%, depending on model conditions. The yields observed in this study suggest that global models discussed above may be substantially overestimating glyoxal production.

In addition, this work demonstrates that even for a molecule that has been as extensively studied as isoprene, its oxidation mechanism is still somewhat uncertain. Although the intramolecular rearrangements as proposed by Dibble (2004a,b) are not likely to correspond to the major channels, they can have a substantial impact on species that are produced in lower concentrations. The results presented here support the existence of such intramolecular rearrangements, which have implications for other

ACPD
11, 10693–10720, 2011

cases for which similar rearrangements have been proposed, including OH recycling (Peeters et al., 2009).

Supplementary material related to this article is available online at: http://www.atmos-chem-phys-discuss.net/11/10693/2011/ acpd-11-10693-2011-supplement.pdf.

Acknowledgements. The authors would like to thank Sam Henry and Dr. Aster Kammrath for instrumental assistance and Dr. Beth Kautzman for help with experimental setup and execution as well as Tzung-May Fu and Jenny Stavrakou for assistance with model comparisons. This work was supported by the National Science Foundation grant ATM–0852406, US Environmental Protection Agency STAR grant RD-833749. It has not been formally reviewed by the EPA. The views expressed in this document are solely those of the authors and the EPA does not endorse any products in this publication.

References

Altieri, K., Seitzinger, S., Carlton, A., Turpin, B., Klein, G., and Marshall, A.: Oligomers formed through in-cloud methylglyoxal reactions: Chemical composition, properties, and mechanisms investigated by ultra-high resolution FT-ICR mass spectrometry, Atmos. Environ., 42, 1476–1490, doi:10.1016/j.atmosenv.2007.11.015, 2008. 10696

Archibald, A. T., Cooke, M. C., Utembe, S. R., Shallcross, D. E., Derwent, R. G., and Jenkin, M. E.: Impacts of mechanistic changes on HO_x formation and recycling in the oxidation of isoprene, Atmos. Chem. Phys., 10, 8097–8118, doi:10.5194/acp-10-8097-2010, 2010a. 10695, 10696

Archibald, A. T., Jenkin, M. E., and Shallcross, D. E.: An isoprene mechanism intercomparison, Atmos. Environ., 44, 5356–5364, doi:10.1016/j.atmosenv.2009.09.016, 2010b. 10696

Carlton, A., Turpin, B., Altieri, K., Seitzinger, S., Reff, A., Lim, H., and Ervens, B.: Atmospheric oxalic acid and SOA production from glyoxal: Results of aqueous photooxidation experiments, Atmos. Environ., 41, 7588–7602, doi:10.1016/j.atmosenv.2007.05.035, 2007. 10696

Carlton, A. G., Wiedinmyer, C., and Kroll, J. H.: A review of Secondary Organic Aerosol (SOA)

formation from isoprene, Atmos. Chem. Phys., 9, 4987–5005, doi:10.5194/acp-9-4987-2009, 2009b. 10696

Chan, A. W. H., Galloway, M. M., Kwan, A. J., Chhabra, P. S., Keutsch, F. N., Wennberg, P. O., Flagan, R. C., and Seinfeld, J. H.: Photooxidation of 2-methyl-3-buten-2-ol (MBO) as a potential source of secondary organic aerosol, Environ. Sci. Technol., 43, 4647–4652, doi:10.1021/es802560w, 2009. 10699, 10703

Cocker, D. R., Flagan, R. C., and Seinfeld, J. H.: State-of-the-art chamber facility for studying atmospheric aerosol chemistry, Environ. Sci. Technol., 35, 2594–2601, doi:10.1021/Es0019169, 2001. 10697

Crounse, J., McKinney, K., Kwan, A., and Wennberg, P.: Measurement of gas-phase hydroperoxides by chemical ionization mass spectrometry, Anal. Chem., 78, 6726–6732, doi:10.1021/ac0604235, 2006. 10698

Dibble, T. S.: Intramolecular hydrogen bonding and double H-atom transfer in peroxy and alkoxy radicals from isoprene, J. Phys. Chem. A, 108, 2199–2207, doi:10.1021/jp0306702, 2004a. 10696, 10697, 10701, 10704, 10707

Dibble, T. S.: Prompt chemistry of alkenoxy radical products of the double H-atom transfer of alkoxyradicals from isoprene, J. Phys. Chem. A, 108, 2208–2215, doi:10.1021/jp0312161, 2004b. 10696, 10697, 10701, 10704, 10707

Ervens, B., Carlton, A. G., Turpin, B. J., Altieri, K. E., Kreidenweis, S. M., and Feingold, G.: Secondary organic aerosol yields from cloud-processing of isoprene oxidation products, Geophys. Res. Lett., 35, L02816, doi:10.1029/2007gl031828, 2008. 10696

Fan, J. and Zhang, R.: Atmospheric Oxidation Mechanism of Isoprene, Environ. Chem., 1, 140–149, doi:10.1071/EN04045, 2004. 10696

Fu, T.-M., Jacob, D. J., Wittrock, F., Burrows, J., Vrekoussis, M., and Henze, D.: Global budgets of atmospheric glyoxal and methylglyoxal, and implications for formation of secondary organic aerosols, J. Geophys. Res., 113, D15303, doi:10.1029/2007JD009505, 2008. 10707

Fu, T.-M., Jacob, D. J., and Heald, C. L.: Aqueous-phase reactive uptake of dicarbonyls as a source of organic aerosol over eastern North America, Atmos. Environ., 43, 1814–1822, doi:10.1016/j.atmosenv.2008.12.029, 2009. 10707

Galloway, M. M., Chhabra, P. S., Chan, A. W. H., Surratt, J. D., Flagan, R. C., Seinfeld, J. H., and Keutsch, F. N.: Glyoxal uptake on ammonium sulphate seed aerosol: reaction products and reversibility of uptake under dark and irradiated conditions, Atmos. Chem. Phys., 9, 3331–3345, doi:10.5194/acp-9-3331-2009, 2009. 10696

Gu, C. L., Rynard, C. M., Hendry, D. G., and Mill, T.: Hydroxide radical oxidation of isoprene, Environ. Sci. Technol., 19, 151–155, doi:10.1021/es00132a007, 1985. 10696

Guenther, A., Hewitt, C., Erickson, D., Fall, R., Geron, C., Graedel, T., Harley, P., Klinger, L., Lerdau, M., Mckay, W., Pierce, T., Scholes, B., Steinbrecher, R., Tallamaraju, R., Taylor, J., and Zimmerman, P.: A global model of natural volatile organic-compound emissions, J. Geophys. Res.-Atmos., 100, 8873–8392, doi:10.1029/94JD02950, 1995. 10695

Henry, S. B., Huisman, A. J., and Keutsch, F. N.: Glyoxal/methylglyoxal as quantified by laser induced phosphorescent decay: methods and results, Atmos. Meas. Tech. Discuss., in preparation, 2011. 10698

Huisman, A. J., Hottle, J. R., Coens, K. L., DiGangi, J. P., Galloway, M. M., Kammrath, A., and Keutsch, F. N.: Laser-induced phosphorescence for the in situ detection of glyoxal at part per trillion mixing ratios, Anal. Chem., 80, 5884–5891, doi:10.1021/ac800407b, 2008. 10698

Huisman, A. J., Hottle, J. R., Galloway, M. M., DiGangi, J. P., Coens, K. L., Choi, W. S., Faloona, I. C., Gilman, J. B., Kuster, W. C., de Gouw, J., Bouvier-Brown, N. C., LaFranchi, B. W., Cohen, R. C., Wolfe, G. M., Thornton, J. A., Docherty, K. S., Farmer, Delphine, K., Cubison, M. J., Mao, J., Brune, W. H., and Keutsch, F. N.: Photochemical modeling of glyoxal at a rural site: observations and analysis from BEARPEX 2007, Atmos. Chem. Phys. Discuss., submitted, 2011. 10697, 10702

Ip, H. S. S., Huang, X. H. H., and Yu, J. Z.: Effective Henry's law constants of glyoxal, glyoxylic acid, and glycolic acid, Geophys. Res. Lett., 36, L01802, doi:10.1029/2008GL036212, 2009. 10696

Jenkin, M. E., Saunders, S. M., Wagner, V., and Pilling, M. J.: Protocol for the development of the Master Chemical Mechanism, MCM v3 (Part B): tropospheric degradation of aromatic volatile organic compounds, Atmos. Chem. Phys., 3, 181–193, doi:10.5194/acp-3-181-2003, 2003. 10696, 10697

Karl, T., Guenther, A., Turnipseed, A., Tyndall, G., Artaxo, P., and Martin, S.: Rapid formation of isoprene photo-oxidation products observed in Amazonia, Atmos. Chem. Phys., 9, 7753–7767, doi:10.5194/acp-9-7753-2009, 2009. 10696

Keywood, M. D., Varutbangkul, V., Bahreini, R., Flagan, R. C., and Seinfeld, J. H.: Secondary organic aerosol formation from the ozonolysis of cycloalkenes and related compounds, Environ. Sci. Technol., 38, 4157–4164, doi:10.1021/Es.035363o, 2004. 10697

Kwok, E. S. C., Atkinson, R., and Arey, J.: Observation of Hydroxycarbonyls from the OH Radical-Initiated Reaction of Isoprene, Environ. Sci. Technol., 29, 2467–2469,

doi:10.1021/es00009a046, 1995. 10696
Loza, C. L., Chan, A. W. H., Galloway, M. M., Keutsch, F. N., Flagan, R. C., and Seinfeld, J. H.: Characterization of vapor wall loss in laboratory chambers, Environ. Sci. Technol., 44, 5074–5078, doi:10.1021/es100727v, 2010. 10702
Madronich, S. and Calvert, J. G.: The NCAR Master Mechanism of the gas phase chemistry-Version 2.0, Rep. NCAR/TN-333+STR, National Center for Atmospheric Research, 1989. 10696, 10697
Miyoshi, A., Hatakeyama, S., and Washida, N.: OH radical-initiated photooxidation of isoprene: An estimate of global CO production, J. Geophys.Res.-Atmos., 99, 18779–18787, doi:10.1029/94JD01334, 1994. 10696
Nozière, B., Dziedzic, P., and Cordova, A.: Products and kinetics of the liquid-phase reaction of glyoxal catalyzed by ammonium ions (NH_4^+), J. Phys. Chem. A, 113, 231–237, doi:10.1021/jp8078293, 2009. 10696
Orlando, J. J., Tyndall, G. S., and Paulson, S. E.: Mechanism of the OH-initiated oxidation of methacrolein, Geophys. Res. Lett., 26, 2191–2194, doi:10.1029/1999gl900453, 1999. 10696, 10702, 10715
Paulot, F., Crounse, J. D., Kjaergaard, H. G., Kroll, J. H., Seinfeld, J. H., and Wennberg, P. O.: Isoprene photooxidation: new insights into the production of acids and organic nitrates, Atmos. Chem. Phys., 9, 1479–1501, doi:10.5194/acp-9-1479-2009, 2009a. 10696, 10697, 10701, 10702, 10704, 10715
Paulot, F., Crounse, J. D., Kjaergaard, H. G., Kurten, A., St. Clair, J. M., Seinfeld, J. H., and Wennberg, P. O.: Unexpected epoxide formation in the gas-phase photooxidation of isoprene, Science, 325, 730–733, doi:10.1126/science.1172910, 2009b. 10698
Paulson, S. E., Flagan, R. C., and Seinfeld, J. H.: Atmospheric photooxidation of isoprene part I: The hydroxyl radical and ground state atomic oxygen reactions, Int. J. Chem. Kin., 24, 79–101, doi:10.1002/kin.550240109, 1992. 10696
Peeters, J., Nguyen, T. L., and Vereecken, L.: HO_x radical regeneration in the oxidation of isoprene, Phys. Chem. Chem. Phys., 11, 5935–5939, doi:10.1039/B908511d, 2009. 10708
Perri, M. J., Seitzinger, S., and Turpin, B. J.: Secondary organic aerosol production from aqueous photooxidation of glycolaldehyde: Laboratory experiments, Atmos. Environ., 43, 1487–1497, doi:10.1016/j.atmosenv.2008.11.037, 2009. 10696
Sareen, N., Schwier, A. N., Shapiro, E. L., Mitroo, D., and McNeill, V. F.: Secondary organic material formed by methylglyoxal in aqueous aerosol mimics, Atmos. Chem. Phys., 10, 997–

1016, doi:10.5194/acp-10-997-2010, 2010. 10696
Saunders, S. M., Jenkin, M. E., Derwent, R. G., and Pilling, M. J.: Protocol for the development of the Master Chemical Mechanism, MCM v3 (Part A): tropospheric degradation of non-aromatic volatile organic compounds, Atmos. Chem. Phys., 3, 161–180, doi:10.5194/acp-3-161-2003, 2003. 10696, 10697
Shapiro, E. L., Szprengiel, J., Sareen, N., Jen, C. N., Giordano, M. R., and McNeill, V. F.: Light-absorbing secondary organic material formed by glyoxal in aqueous aerosol mimics, Atmos. Chem. Phys., 9, 2289–2300, doi:10.5194/acp-9-2289-2009, 2009. 10696
Sprengnether, M., Demerjian, K. L., Donahue, N. M., and Anderson, J. G.: Product analysis of the OH oxidation of isoprene and 1,3-butadiene in the presence of NO, J. Geophys. Res., 107, 4268, doi:10.1029/2001jd000716, 2002. 10696
St. Clair, J. M., McCabe, D. C., Crounse, J. D., Steiner, U., and Wennberg, P. O.: Chemical ionization tandem mass spectrometer for the in situ measurement of methyl hydrogen peroxide, Rev. Sci. Instrum., 81, 094102–094106, doi:10.1063/1.3480552, 2010. 10698
Stavrakou, T., Müller, J.-F., De Smedt, I., Van Roozendael, M., Kanakidou, M., Vrekoussis, M., Wittrock, F., Richter, A., and Burrows, J. P.: The continental source of glyoxal estimated by the synergistic use of spaceborne measurements and inverse modelling, Atmos. Chem. Phys., 9, 8431–8446, doi:10.5194/acp-9-8431-2009, 2009. 10707
Tan, Y., Perri, M. J., Seitzinger, S. P., and Turpin, B. J.: Effects of precursor concentration and acidic sulfate in aqueous glyoxal-OH radical oxidation and implications for secondary organic aerosol, Environ. Sci. Technol. 43, 8105–8112, doi:10.1021/es901742f, 2009. 10696
Taraborrelli, D., Lawrence, M. G., Butler, T. M., Sander, R., and Lelieveld, J.: Mainz Isoprene Mechanism 2 (MIM2): an isoprene oxidation mechanism for regional and global atmospheric modelling, Atmospheric Chemistry and Physics, 9, 2751–2777, doi:10.5194/acp-9-2751-2009, 2009. 10696, 10697
Tuazon, E. C. and Atkinson, R.: A product study of the gas-phase reaction of methyl vinyl ketone with the OH radical in the presence of NO_x, International Journal of Chemical Kinetics, 21, 1141–1152, doi:10.1002/kin.550211207, 1989. 10696, 10702, 10715
Tuazon, E. C. and Atkinson, R.: A product study of the gas-phase reaction of isoprene with the OH radical in the presence of NO_x, International J. Chem. Kin., 22, 1221–1236, doi:10.1002/kin.550221202, 1990a. 10696, 10701, 10715
Tuazon, E. C. and Atkinson, R.: A product study of the gas-phase reaction of methacrolein with the OH radical in the presence of NO_x, International J. Chem. Kin., 22, 591–602,

ACPD
11, 10693–10720, 2011

High–NO_x VOC oxidation yields

M. M. Galloway et al.

doi:10.1002/kin.550220604, 1990b. 10696, 10702, 10715

Volkamer, R., Barnes, I., Platt, U., Molina, L. T., and Molina, M. J.: Remote sensing of glyoxal by differential optical absorption spectroscopy (DOAS): Advancements in simulation chamber and field experiments, in: Environmental Simulation Chambers: Application to Atmospheric Chemical Processes, edited by: Barnes, I. and Rudinski, J., 62, Springer, Dordrecht, Netherlands, 2006. 10696, 10697, 10701

Volkamer, R., Ziemann, P. J., and Molina, M. J.: Secondary organic aerosol formation from acetylene (C_2H_2): seed effect on SOA yields due to organic photochemistry in the aerosol aqueous phase, Atmos. Chem. Phys., 9, 1907–1928, doi:10.5194/acp-9-1907-2009, 2009. 10696

Zhao, J., Zhang, R., Fortner, E. C., and North, S. W.: Quantification of Hydroxycarbonyls from OHIsoprene Reactions, J. Am. Chem. Soc., 126, 2686–2687, doi:10.1021/ja0386391, 2004. 10696

ACPD

11, 10693–10720, 2011

High–NO_x VOC oxidation yields

M. M. Galloway et al.

Table 1. Experiment list.

Exp. #	Date (mm/dd/yy)	Compound	Initial conc. (ppb)	Initial NO (ppb)	RH (%)	*T* (K)	Lights	OH source
C1	02/06/08	Glyoxal	499	3	3	298	50%	None
1	07/21/10	Glyoxal	64	3	4	294	50%	None
2	02/02/08	Isoprene	603	466	4	293	10%	HONO
3	02/04/08	Isoprene	609	465	5	294	10%	HONO
4	10/15/09	Isoprene	187	361	8	295	10%	HONO
5	10/17/09	Isoprene	17	250	9	295	10%	HONO
6	10/19/09	Isoprene	187	307	10	294	10%	HONO
7	07/22/10	Isoprene	60	325	4	293	10%	HONO
8	10/21/09	MVK	25	279	10	295	10%	HONO
9	07/20/10	MVK	20	294	4	294	10%	HONO
10	10/23/09	MACR	42	231	7	295	10%	HONO
11	10/25/09	Blank	None	250	8	294	10%	HONO

ACPD
11, 10693–10720, 2011

Table 2. first-generation yields from high NO_x experiments. All yields and errors are in percent. The MCM yields are calculated for the reaction with OH and on the basis that the fate of peroxy radicals is dominated by NO with negligible contribution from reaction with HO_2 or RO_2.

Compound	MVK	MACR	Glycolaldehyde	Hydroxyacetone	Glyoxal	Methylglyoxal
Isoprene	29.7 ± 1.7%	23.3 ± 2.1%	2.7 ± 1.0%	$2.58_1 \pm 0.04_7$%	$2.0_7 \pm 0.3_0$%	ND
Isoprene[a]	29 ± 7%	21 ± 5%				
Isoprene[b]	40%	26%	4.2%	3.8%	[h]3.8%	[h]4.2%
Isoprene[f]	34.2%	22.2%	NI	NI	NI	NI
MVK			$72.1_3 \pm 0.9_8$%	[g]0%	[g]0%	$27.2_8 \pm 0.1_3$%
MVK[c]			64 ± 8%	25 ± 4%		
MVK[b]			62.5%	[h]26.5%		
MVK[f]			70%	NI	NI	29%
MACR			[g]0%	$44.0_2 \pm 0.2_3$%	[g]0%	$3.5_1 \pm 0.2_7$%
MACR[d]				41 ± 3%		8.4 ± 1.6%
MACR[e]				47 ± 5%		<12%
MACR[b]				20%		[h]0%
MACR[f]			NI	43%	NI	NI

ND = no data.
NI = not included in the MCM.
[a] Tuazon and Atkinson (1990a).
[b] Paulot et al. (2009a).
[c] Tuazon and Atkinson (1989).
[d] Tuazon and Atkinson (1990b).
[e] Orlando et al. (1999).
[f] MCM
[g] 0% within uncertainty of measurement.
[h] Inferred from the presented mechanism from that study.

ACPD
11, 10693–10720, 2011

Table 3. Total molar yields from isoprene oxidation with OH calculated with the modified MCM for high NO_x conditions.

Compound	Total Yield
MVK	35.7%
MACR	22.4%
Glycolaldehyde	15.7%
Hydroxyacetone	15.8%
Glyoxal	6.30%
Methylglyoxal	29.0%

ACPD
11, 10693–10720, 2011

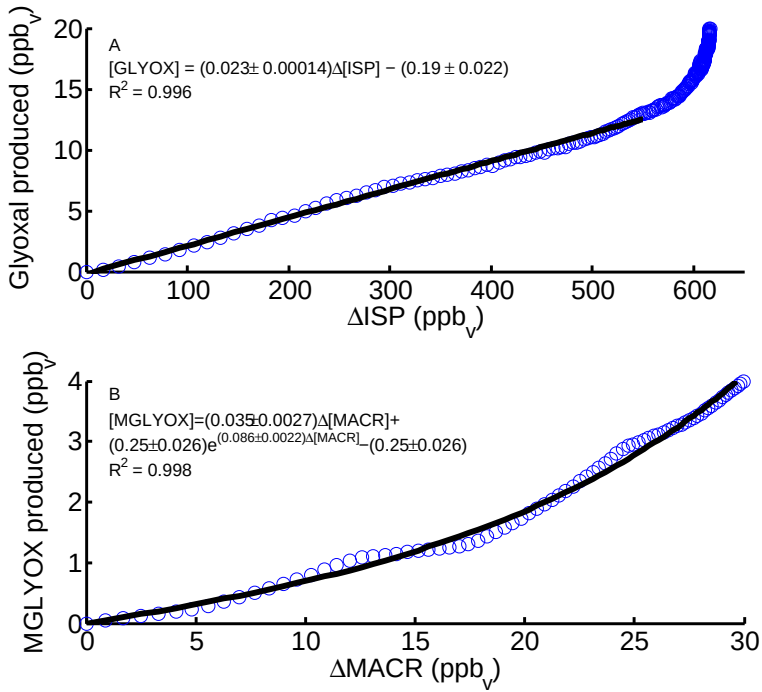

Fig. 1. (A) Glyoxal production as a function of isoprene reacted in Exp. 2. Note the linear relationship between glyoxal and isoprene reacted in the first part of the experiment. The continued upward trend in glyoxal after isoprene is consumed corresponds to the formation of glyoxal as a higher generation oxidation product. **(B)** Methylglyoxal production as a function of MACR reacted in Exp. 10.

ACPD
11, 10693–10720, 2011

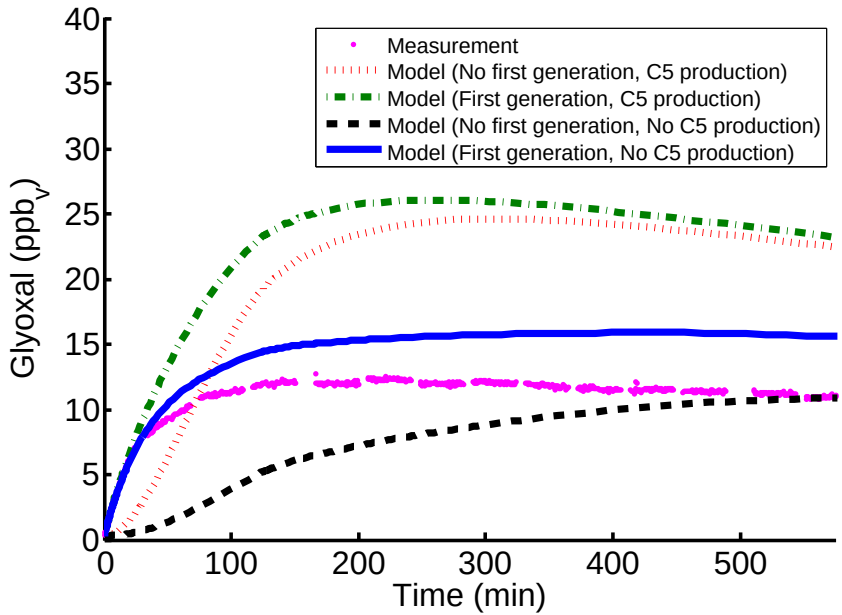

Fig. 2. Comparison of measured glyoxal concentration and MCM prediction for Exp. 2. Attenuation of glyoxal production from C5 carbonyls brings the model into closer agreement with measurement during the latter part of the experiment.

ACPD
11, 10693–10720, 2011

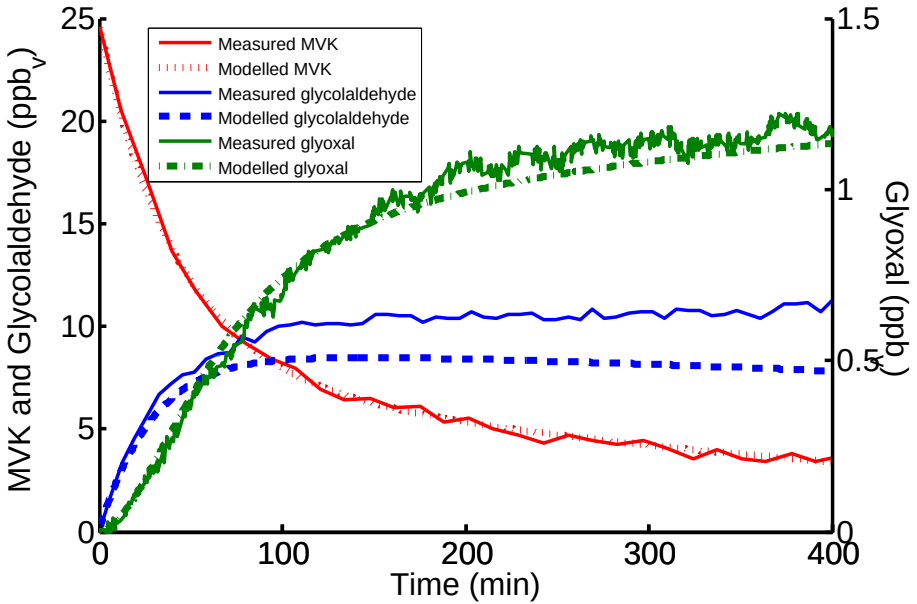

Fig. 3. Model and measurement comparison for high NO_x MVK oxidation (Exp. 8).

ACPD
11, 10693–10720, 2011

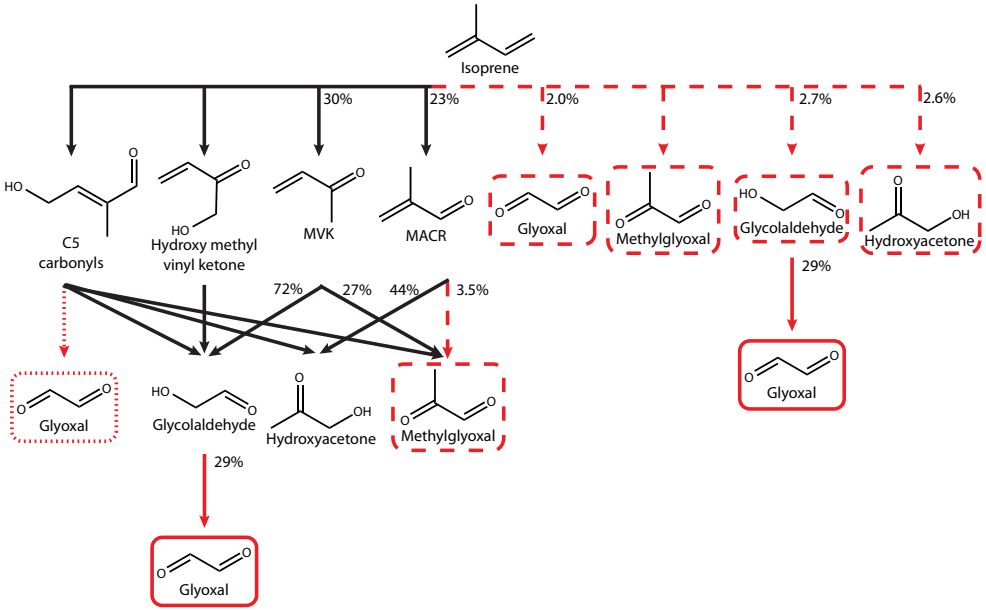

Fig. 4. Isoprene oxidation scheme. Dashed lines indicate first-generation formation pathways not included in the MCM. Dotted lines indicate pathways attenuated in our modelling studies. Yields given are those found in this study.

ACPD
11, 10693–10720, 2011